Polymer Degradation and Stability 181 (2020) 109333

Contents lists available at ScienceDirect

Polymer Degradation and Stability

journal homepage: www.elsevier.com/locate/polymdegradstab

Recalcitrance of hair in historical plasters

J. Tintner[a], H. Rennhofer[a,*], C.J. Kennedy[b], W.A. Revie[c], H. Weber[a], C. Pavlik[a], J. Lanszki[d]

[a] University of Natural Resources and Life Sciences, Institute of Physics and Materials Science, Peter Jordan Straße 82, 1190-Vienna, AT, Austria
[b] Heriot Watt University, School of Energy, Geoscience, Infrastructure and Society, Edinburgh, Scotland EH14 4AS, UK
[c] Construction Materials Consultants, Wallace House, Whitehouse Road, Stirling, Scotland FK7 7TA, UK
[d] Kaposvár University, Institute of Environmental Sciences and Nature Conservation, Kaposvár, P.O. Box 16, 7400 Hungary

ARTICLE INFO

Article history:
Received 10 January 2020
Revised 20 July 2020
Accepted 11 August 2020
Available online 12 August 2020

Keywords:
Lime plaster
Animal hair
Amendment
FTIR spectroscopy
Small-angle X-ray scattering SAXS

ABSTRACT

Hair amendments were extracted from the lime plasters of historical buildings with an age ranging from recent times until the 12th century. Infrared spectroscopy has been used to assess chemical changes, small-angle X-ray scattering (SAXS) for changes of the physical structure. As a reference a sample set of 130 recent samples has been collected comprising different species. The only strong impact on hair chemistry was detected for grinding the samples. This pretreatment separated the chemical fingerprint based on methylene bands (2920 and 2850 cm^{-1}) and the C=O vibration band at 1740 cm^{-1}. Different species were separated only on a coarse level. Historical samples did not display very clear indicators of aging processes. SAXS results registered a certain grouping of the samples according to age. A clear trend was not found, however. This suggests that age alone is not the key defining factor in the degradation processes in hair.

1. Introduction

Hair in plasters and mortars has been a common reinforcement for many centuries [1,2]. It improves tensile strength and helps to reduce shrinkage fissures and cracks [3]. In comparison to straw the amendment of hair leads to a smoother surface. It is important to understand the decay processes that cause hair-reinforced lime plasters to fail over time.

Molecular decay measured by means of Fourier Transform Infrared (FTIR) spectroscopy in organic materials is a rising issue in the field of archaeometry. It has been used to investigate production conditions of charcoal [4] and to characterize historical paper [5]. Hairs are among the most prominent human relicts under specific preservation conditions [6,7]. Chemically, hair consists mainly of keratin, a water-insoluble fibrous protein. Morphologically, hair consists of three layers with a thin cuticula as surface layer, a large cortex bearing the highest mass proportion and often a centrally-located medulla [8]. Natural degradation is based on mainly bacterial and fungal enzymatic reactions [9,10].

FTIR and Small-angle X-ray Scattering (SAXS) are well established methods for the chemical and physical characterization of various materials, like charcoal [11], wood [12,13], antler [14], bone [15,16] and hair [17]. The methods combine the advantages of high speed and a minimum of sample preparation with high information content. They are also complementary; FTIR assesses any chemical changes in the molecular structure of keratin, whilst SAXS is used to understand structural alterations on a hierarchical level.

The objective of this work was the characterization of historical hair in plasters by means of FTIR spectroscopy and SAXS with the specific goal to identify any potential degradation processes that can be used to predict age. Acting as a basis of that work we investigated the homogeneity of hair originating from different species and we compared different sample preparations.

2. Material and methods

2.1. Material

To compare the historical samples with recent ones, we sampled 125 fresh hair samples from different species. Variability within the species was covered especially for human hair. Female and male hair was covered, age of people ranged from 3 to 95 years. Very different colors and even hair treatments were covered,

* Corresponding author.
E-mail addresses: johannes.tintner@boku.ac.at (J. Tintner), harald.rennhofer@boku.ac.at (H. Rennhofer), craig.Kennedy@hw.ac.uk (C.J. Kennedy), billrevie@cmcstirling.co.uk (W.A. Revie), christianpavlik@gmx.at (C. Pavlik), lanszkij@gmail.com (J. Lanszki).

https://doi.org/10.1016/j.polymdegradstab.2020.109333

Table 1
List of 125 reference materials.

Species	Milled	Original
Human, male	13	7
Human, female	20	10
Goat	1	0
Dog	8	6
Cat	5	4
Horse	5	9
Donkey	2	1
Cow	1	5
Boar	1	13
Deer	2	9
Rat	0	2
Badger	0	1

Table 2
Origin and year of the hair samples from historical plasters.

Location	Country	Age (AD)
Vienna	Austria	2017
Hope Lodge, Sutherland	Scotland	1878
Moccas Court, Herefordshire	England	1780
Malton, North Yorkshire	England	1682
York House, Malden	England	1682
Stetteldorf, Lower Austria	Austria	1610
Pond Farmhouse, York	England	1580
St. Georgen, Upper Austria	Austria	1168
Agatunet, Hardanger	Norway	1495 (1465-1524)

as well. Animal hair was sampled more or less randomly. A compilation of the samples is given in Table 1.

Historical plaster samples originated from different buildings of differing ages from across Europe. Origin and age of these samples are given in Table 2. From each single location one sample consisting of several hairs could be obtained. The ages of the samples were given by archaeologists who took the samples with dating based on historical records. The exception to this is the sample Agatunet, Hardanger which was initially dated to the 11^{th}–12^{th} century, but subsequent radiocarbon dating (data not shown) has indicated it dates from AD 1465 to 1524. To simplify the figures, we indicate the sample there with the median – AD 1495. Sampling was performed in the course of renovation tasks. All plasters except one were lime plasters. Based on XRD analyses (not performed within this project) calcite amounted for 85–95% $_{mass}$ with little amendments of gypsum and quartz. Only the sample from Agatunet, Hardanger, Norway originated from a clay mortar containing different clay minerals (40% $_{mass}$), quartz (25%), plagioclase (22%), sanidine (11%), and amphibole (2%). All samples with the exception of the sample from Agatunet, Norway and St. Georgen, Upper Austria, which were both sampled from north facings outside of the respective buildings, were sampled from internal walls of complete buildings. However, given the age and condition of the buildings it is likely, with the exception of perhaps Moccas Court, Herefordshire, and Stetteldorf, Lower Austria, that they experienced extended periods where the walls would have been affected by dampness, either through water penetration and/or high levels of humidity.

2.2. Methods

2.2.1. Sample preparation

Around half of the reference samples has been powdered with a steel disc vibratory mill (Fritsch Pulverisette 9). Around 100 to 500 mg were milled between 30 and 120 s with 1000 rpm. Historical plasters were soaked in water for 10–12 h, dispersed manually and hairs picked out with tweezers. Afterwards they were treated by an acetate buffer to destroy calcite remains and washed under water. This treatment is known to keep the impact on the sample gentle. In soil analyses acetate buffer results in extraction rates comparable to water [18]. All samples (even the fresh ones) were dried at 65 °C before measurement. This temperature results in the removal of adjacent water, but not in structural changes of keratin [19,20]. It is evident that the indicative value of the water content regarding degradation effects was levelled, but as samples had to be washed, drying was unavoidable. At least, the process was similar for all samples.

2.2.2. Fourier Transform Infrared (FTIR) spectroscopy and statistical evaluation

FTIR spectra were recorded in the ATR (attenuated total reflection) mode in the mid infrared range (4000–400 cm^{-1}) with an optical crystal of a Bruker ® Helios FTIR micro sampler (Tensor 27). This device allows spot measurements with a spatial resolution of 250 micrometer. 32 scans were recorded at a spectral resolution of 4 cm^{-1}. Five replicate measurements per sample have been performed. Spectra were vector normalized and the replicates averaged using the OPUS © (version 7.2) software. Principal Component Analysis (PCA) has been performed using The Unscrambler X 10.1 © Camo. Wavenumber regions included the spectral regions from 3722 cm^{-1} to 2422 cm^{-1} and from 1875 cm^{-1} to 400 cm^{-1}. Excluded wavenumber regions are affected by disturbing signals of the diamond crystal.

2.2.3. Small angle X-ray scattering (SAXS)

SAXS images were recorded with a RIGAKU S-Max 3000 machine with a MM002+ Cu microfocus tube (wavelength $\lambda = 0.154$ nm) and Triton200 ® multiwire detector in a range of the scattering vector from about 0.1 nm^{-1}–8 nm^{-1}. Several hairs have been placed in a polymer envelope and measured in vacuum. Scattering images were integrated in order to obtain intensity I(q) as a function of the length of the scattering vector q, which is related to the wavelength λ and the scattering angle 2θ by the Braggs law: $q = \frac{4\pi}{\lambda} sin\theta$. The scattering curves I(q) were background corrected and subjected to further data evaluation.

2.2.4. Scanning electron microscopy (SEM)

For the SEM investigations a FEI Quanta 250 FEG (Thermo Fisher Scientific ®, Hillsboro, OR) was used under high vacuum condition. The micrographs were recorded with the Everhart-Thornley-Detector in secondary electron (SE) mode and a high tension of 20 kV. The specimens were mounted with conductive double sided carbon tape on an aluminium stub with five centimeter diagonal that was sputtercoated with a 10 nm thin layer of gold and Argon atmosphere in a Scancoat six (Edwards ®, Burgess Hill, UK) in order to provide sufficient electrical conductivity.

2.2.5. Light microscopic hair identification

To study the cuticular pattern of historical hair samples, a thin layer of warm 10% gelatin stock solution was brought onto a slide, and then the selected hair samples were placed on the surface [21]. After drying the gelatin film, the hairs were removed and the imprints were examined under a light microscope (400x magnification). To study the medullar hair pattern, hair samples were fixed on a slide with small drops of glue (colorless nail polisher) at a number of points. When the glue has hardened, hairs were cut between the glue drops, and then hairs were mounted with paraffin oil. Medullar pattern was examined under 100 to 400x magnification. For hair identification, keys [21–23] and reference hair collection was used.

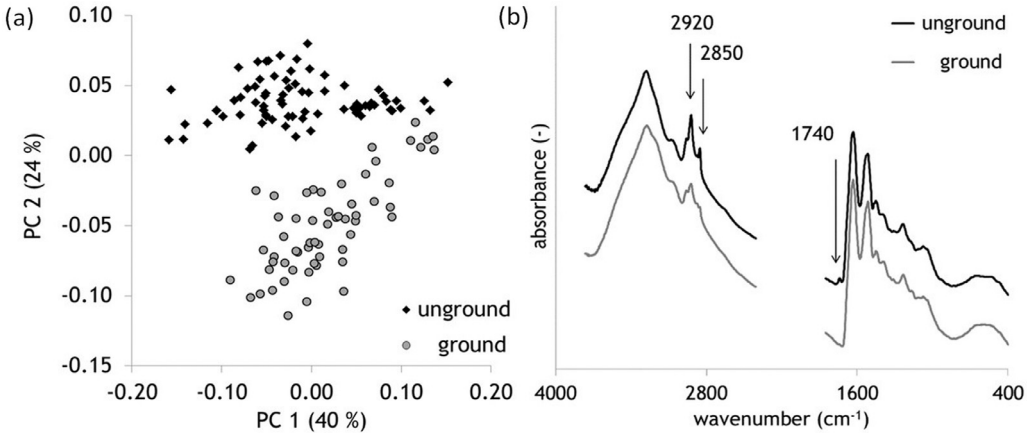

Fig. 1. (a) Scores of PCA, (b) average spectra of ground and unground samples, n=134.

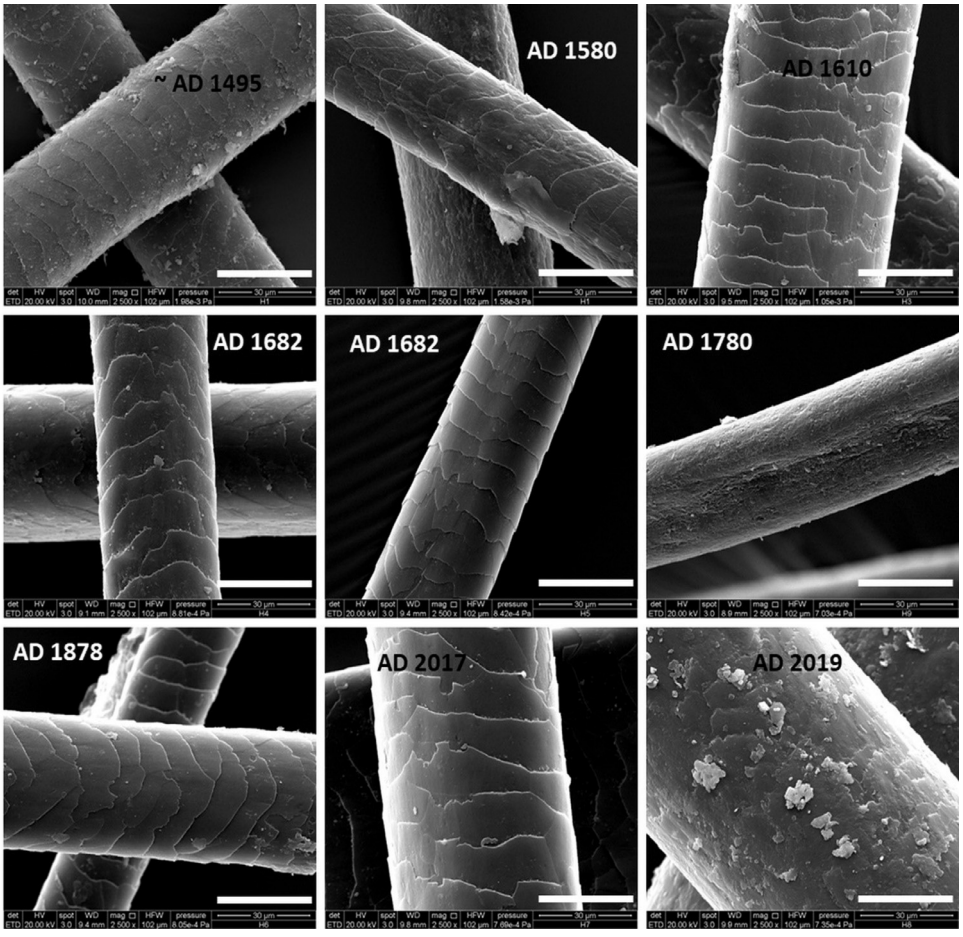

Fig. 2. SEM-pictures of historical hair samples, magnification 2500 times, white bar at the right bottom corner represents 30 μm; ages given in the pictures decrease from top left (~AD 1495) to the recent reference at bottom right (AD 2019).

3. Results

3.1. Recent samples

PCA based on FTIR spectra for the whole sample set revealed significant differences for ground samples. PC1 structures heterogeneity among different species and accounts for 40% of data variability. PC2 separates ground samples from unground, original samples and accounts for 24% of data variability (Fig. 1a). Unground samples revealed more prominent methylene bands with maxima at 2920 and 2850 cm^{-1}. Furthermore a small but conspicuous band at 1740 cm^{-1} is visible that stays absent in the ground spectra (Fig. 1b). The band can be assigned to carbonyl C=O stretch vibration e.g. in saturated esters [24].

3.2. Assessment of historical hair samples

Fig. 2 presents SEM pictures of the historical samples with intact cuticular structures with the exception of sample AD 1780 with a smoother surface.

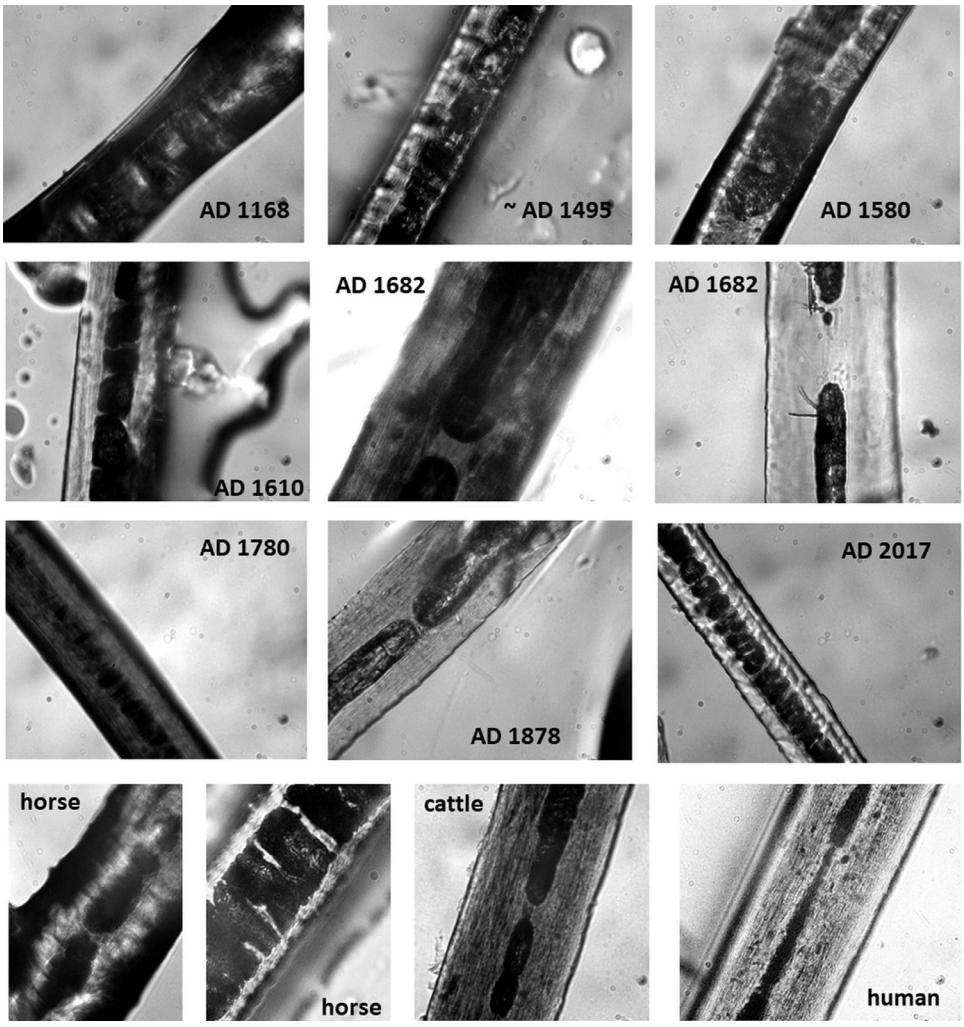

Fig. 3. Light microscopic pictures of historical hair samples, magnification 400 times; ages given in the pictures, the four pictures in the lowest row represent recent reference samples of different animal species

Table 3
Power law exponent *n* indicating roughness of interfaces. Error from the fit is about $\Delta n = 0.02$. Animal species information based on light and electron microscopic analyses.

Sample	*Power law exponent n*	*Animal species*
AD 1168	3.64	Horse
AD 1465-1525	3.79	Horse
AD 1580	3.66	Horse
AD 1610	3.51	Horse
AD 1682	3.78	Cattle
AD 1682	3.78	Cattle
AD 1780	3.68	Horse
AD 1878	3.77	Cattle and horse
AD 2017	3.83	Horse
AD 2019	3.86	Cattle

Based on light microscopic analyses of cuticular and medullar patterns of hairs (Fig. 3), most historical samples originated from horse, in some cases from cattle, and mixed hairs of these two species were also found (species were added in Table 3).

All historical samples were measured by means of FTIR unground and were situated intermingled within the group of unground samples. Therefore, a PCA was calculated including only unground samples. Results are given in Fig. 4.

Scores plot in Fig. 2a revealed systematic differences among hair of different species, even if many species are considerably intermingled. On the right side of the plot deer, dog, and cat hair is concentrated. On the lower left corner wild boar hair is grouped. Horse and human hair can be found in between these groups. Anyhow, the groups clearly overlap indicating that inner-species variability is considerably high. The main bands reasoning separation along with PC 1 are amide I, I and to some extent amide III with maxima at 1640, 1540, and 1265 cm^{-1}. PC 2 is dominated by methylene band maxima at 2920 and 2850 cm^{-1} plus a certain maximum at 1740 cm^{-1} (Fig. 4b).

To assess historical samples in detail FTIR spectra of the nine samples plus an additional recent reference are presented in Fig. 5.

FTIR spectra of the different historical samples did not display any systematic trend in any band region. In fact, there are several slight differences between them, but samples with very different ages display comparable band shapes. There are some samples with a convex shoulder on the left arm of the broad band assigned to OH ranging from 3600 to 3100 cm^{-1}, e.g. AD 1465-1524 and AD 1610. Methylene bands displayed sharper maxima in the reference of AD 2019 and the sample from AD 1780. Interesting behavior has been found at the band around 1035 cm^{-1} marked by a vertical line. The band arose in the reference as well as the samples from AD 1780, one from AD 1682, and AD 1465-1524. This band can be related to the sulfoxide (S=O) bond [24] and cysteic acid. This can be an indication of polypeptide chain depolymerization [17].

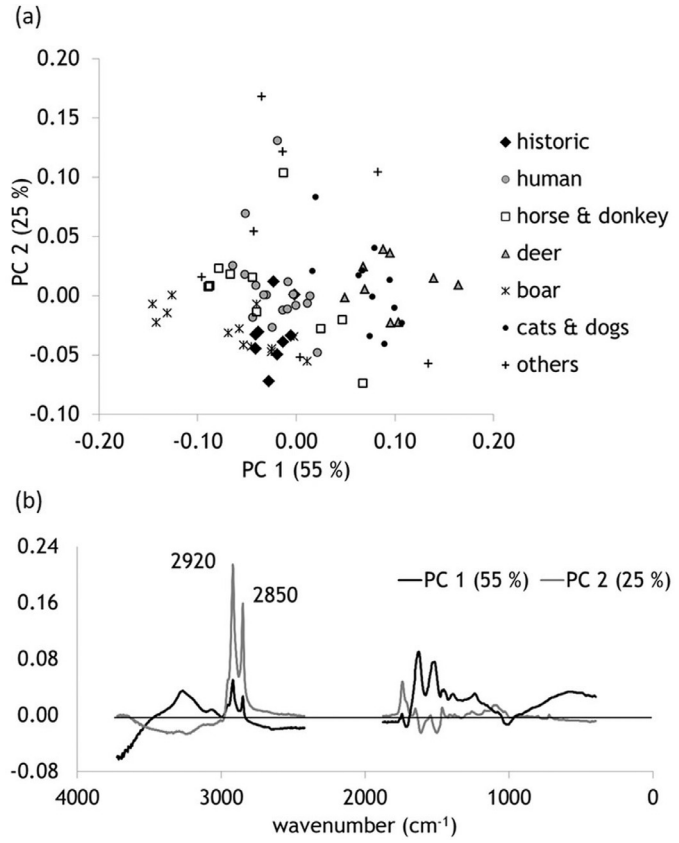

Fig. 4. (a) Scores and (b) Loadings plot of PCA containing only unground samples n=81.

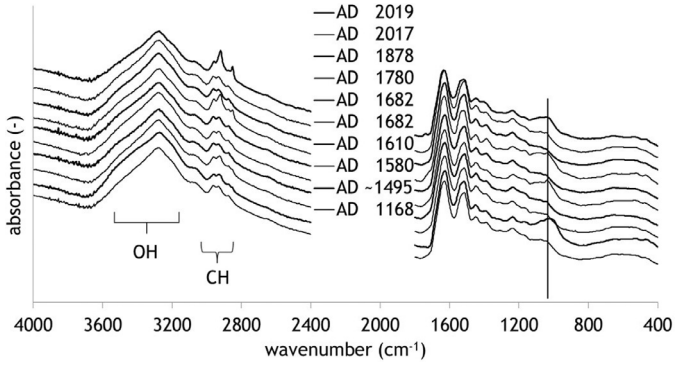

Fig. 5. FTIR spectra of the nine historical hair samples plus a reference sample from 2019, spectra shifted along the y-axis, vertical line indicates band position 1035 cm^{-1}.

Small angle scattering shows typical features for hair, i.e. a peak around q = 0.8 nm^{-1}, which is attributed to the inter-filament distance and for some samples a peak around q = 1.5 nm^{-1}, which is attributed to lipid crystals [17,25]. The inter-filament distance would be about 7.8 nm. Besides this a power law behavior $I(q) \sim q^{-n}$ towards low-q values is observed, where the exponent n can be related to the roughness of interfaces in the nm-structures [26]. Smooth interfaces would show a value of n = 4 and rougher surfaces values towards n = 3. Furthermore all spectra feature a rather amorphous shoulder around q = 7 nm^{-1}, which could be related to the amorphous phase embedding the crystalline filaments. The spectra can be found in Fig. 6.

There are several differences between the individual spectra, i.e. the shape and height of the inter-filament distance peak, or presence of the lipid related peak, which do not allow a clear relation between structure features and age. Nevertheless some differences exist between younger samples and very old samples (older than 1600 AD). Samples AD 1465-1524, AD 1168 and AD 1580 do not show a clear inter-filament distance peak, which is otherwise visible in all samples of newer date, with respect to the sample AD 1780, which also does not show such a peak. These samples do show a rather broad shoulder, which indicates a wide distribution of distances.

The power law exponent of the samples was evaluated in the q range of 0.13–0.3 nm^{-1}. Values of the power law exponent can be found in Table 3. The power law exponent shows rather smooth interfaces with values around 3.8 for recent samples and decreasing values with increasing age, e.g. n = 3.64 for AD 1168.

The amorphous shoulder at 7 nm^{-1} and the lipid related peak at 1.5 nm^{-1} do not show a trend with age.

4. Discussion

Results of grinding revealed obvious differences in methylene bands and carbonyl groups that can be assigned to saturated esters. These esters do not derive from keratin, but could be assigned to wax esters in sebaceous gland lipids [27,28] that can be attached to the hair surface systematically in comparison to the inner surface. McMullen et al. [29] display infrared spectra from the three layers of hair cross sections – cuticula, cortex and medulla. They show the sharpest methylene bands for medulla areas, but no band at the position 1740 cm^{-1} in any of these regions.

Within the samples of human hair there was no systematic difference detectable regarding age or sex. Machado et al. [30] investigated skin by means of ATR-FTIR and did not detect significant differences in terms of age and sex. These results are extended by our study to hair. Corresponding results for hair have been found by Pienpinijtham et al. [31]. Different species were separated to some extent by infrared spectra mainly by the intensity of amide I, II and III bands. Espinoza et al. [32] reported systematic differences in elephant hair linked to the stronger presence cysteid acid.

Historical samples revealed no systematic, significant changes over time, but anyhow show certain differences between very old samples (e.g. AD 1168) and more recent samples (e.g. AD 1682, AD 2017). Neither abiotic aging effects nor effects due to the high pH value in lime plaster starting on a level of pH 12 led to shifts in PCA. SAXS clearly shows that interfaces become rougher, as indicated by the decreasing value for the power law exponent. This hints to a deterioration of interfaces, between e.g. supramolecular structures and disordered material, which does affect the SAXS signal related to the inter-filament distance. Indeed very old samples show no clear inter-filament distance peak. This could indicate a change in the morphology towards a less ordered and less pronounced structure, originating from decay. For recent Yak hair a value of n = 4.0 was reported, but change with treatment or age was not investigated in this context [33]. Also sample AD 1780 shows absence of the inter-filament distance peak and a rather small value for the power law exponent (n = 3.68). Different scenarios could attribute to this, possibly more aggressive storage environment, additional treatment before application or decay before application of the hair. On the other hand sample AD 1465-1524 does show an absent inter-filament peak, but a rather high value for the power law exponent, sample AD 1610 shows an inter-filament peak, but a very low value for the power law exponent. These findings indicate that different decay or preservation mechanisms might be involved. It should be mentioned that sample pre-treatment, in general, bears the risk of leveling degradation markers, e.g. by removing degradation products. We kept the pre-treatment steps to a minimum, so pH was stabilized by an acetate buffer – a very gentle treatment in comparison to the extremely high pH during lime plastering. Also the temperature was

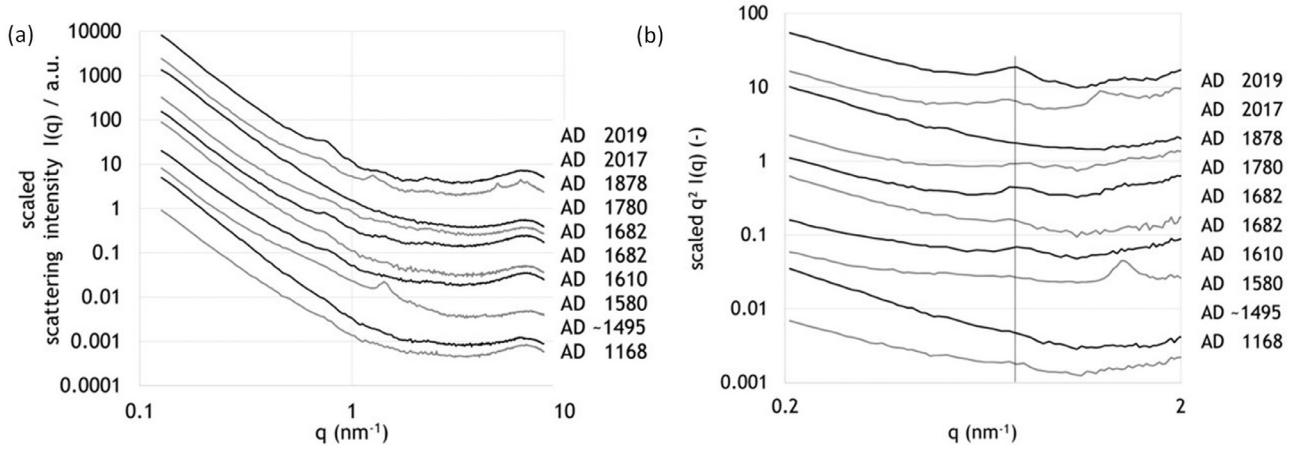

Fig. 6. (a) Small angle scattering curves; (b) Kratky plot $q^2 \bullet I(q)$ as a function of the scattering vector q for the region around the inter-filament peak at about 0.8 nm^{-1}.

kept moderate with 65 °C avoiding any structural changes arising at higher temperatures above 100 °C [19,20]. Anyhow, certain weak effects of our pre-treatment cannot be excluded completely. Other biomacromolecules suffer certain structural changes over time, even within a comparable short time. Structural deterioration has been observed in paper within decades [34], in wood within centuries [35]. Effects of low pH-treatment on hair have been observed by Kennedy et al. [17]. They report an increase of cysteic acid by the oxidation of cysteine after low pH-treatment. Istrate et al. [36] demonstrated an increase of thermal stability of alpha-keratins after a low pH-treatment. Obviously preservation conditions in plasters lead to negligible degradation processes. Diverse preservation statuses have been reported for Egyptian mummies dependent on mummification techniques [37] ranging from almost unaffected to highly porous hair with strongly damaged cuticula. The band around 1035 cm^{-1} probably plays a major role in terms of hair degradation. The formation of cysteic acid is described as a matter of degradation in historical wool in Tudor tapestries [38]. Also the sulfoxide bond due to S-S bond breaking occurs in the same spectral region. It can be seen as a first step of biodegradation followed by the formation of cysteic acid [39]. Interestingly, SEM pictures presented there display very obvious markers of fungal attack. Such markers were not found in our samples. We can assume that the visible increase of the band around 1035 cm^{-1} is linked to certain degradation processes. As the band does not increase in direct correlation with age, it could be possible that these degradation processes already occurred before the material has been put into the plasters. The band cannot be used as a proxy for the estimation of age of unknown samples. It would be interesting to address the question of age determination by other methods like racemization of aspartic acid [40].

5. Conclusion

Infrared spectra, small angle X-ray scattering curves, and electron microscopic pictures carried out on hair samples from historical plasters revealed no significant systematic aging effect over a time period of about 800 years, but only some indication on morphological changes with long aging periods. We conclude that hair in general stays quite unaffected by shorter time depending processes and that longer time influence might include several decay processes. The analyses of a broad reference set unveiled differences in FTIR spectra of recent hair from different species, but also broad overlaps. Only milling the hair was found to generate systematic changes in the spectral pattern. Unground hair sampled displayed strong bands of methylene and around 1740 cm^{-1} that could indicated saturated esters of waxes produced by sebaceous glands.

Funding

Open access funding provided by University of Natural Resources and Life Sciences Vienna (BOKU)

Declaration of Competing Interest

The authors declare that they have no known competing financial interests or personal relationships that could have appeared to influence the work reported in this paper.

CRediT authorship contribution statement

J. Tintner: Conceptualization, Methodology, Investigation, Formal analysis, Writing - original draft, Writing - review & editing. **H. Rennhofer:** Conceptualization, Methodology, Investigation, Formal analysis, Writing - original draft, Writing - review & editing. **C.J. Kennedy:** Resources, Writing - review & editing. **W.A. Revie:** Resources, Writing - review & editing. **H. Weber:** Resources, Formal analysis, Investigation. **C. Pavlik:** Resources, Formal analysis, Investigation. **J. Lanszki:** Resources, Formal analysis, Investigation, Visualization.

Acknowledgements

We thank Leon Ploszczanski for ESEM analyses. We thank diocese Linz, the parish St. Georgen/ Obernberg, and Georg Stradiot for sampling permission and Maria Frieberger-Ernetzl for assistance during sampling. We thank Beate Sipek (Academy of Fine Arts) and Robert Linke (Federal Monuments Authority Austria) for sample information and samples. Thanks to numerous people for recent hair samples, especially Forstverwaltung Kleinmariazell and Jennifer Hatlauf for animal hair.

References

[1] W. Millar, Plastering: plain and decorative, London, New York, 1899.
[2] R. Nogueira, A.P. Ferreira Pinto, A. Gomes, Cem. Concr. Compos. 89 (2018) 192–204.
[3] T. Ashour, A. Derbala, Agric. Eng. Int. CIGR J. 12 (2010) 55–62.
[4] E. Smidt, J. Tintner, S. Klemm, U. Scholz, Quaternary Int. 457 (2017) 43–49.
[5] T. Trafela, M. Strlič, J. Kolar, D.A. Lichtblau, M. Anders, D.P. Mencigar, B. Pihlar, Anal. Chem. 79 (2007) 6319–6323.
[6] R. Bonnichsen, L. Hodges, W. Ream, K.G. Field, D.L. Kirner, K. Selsor, R.E. Taylor, J. Archaeol. Sci. 28 (2001) 775–785.
[7] S. Karodia, J.I. Phillips, A.B. Esterhuysen, J. Archaeol. Sci. 6 (2016) 24–34.

[8] J.L. Woods, D.P. Harland, J.A. Vernon, G.L. Krsinic, R.J. Walls, J. Morphol. 272 (2011) 34–49.
[9] S. Yamamura, Y. Morita, Q. Hasan, S.R. Rao, Y. Murakami, K. Yokoyama, E. Tamiya, J. Biosci. Bioeng. 93 (2002) 595–600.
[10] S. Yamamura, Y. Morita, Q. Hasan, K. Yokoyama, E. Tamiya, Biochem. Biophys. Res. Commun. 294 (2002) 1138–1143.
[11] J. Tintner, C. Preimesberger, C. Pfeifer, D. Soldo, F. Ottner, K. Wriessnig, H. Rennhofer, H. Lichtenegger, E.H. Novotny, E. Smidt, Ind. Eng. Chem. Res. 57 (2018) 15613–15619.
[12] J. Färber, H.C. Lichtenegger, A. Reiterer, S. Stanzl-Tschegg, P. Fratzl, J. Mater. Sci. 36 (2001) 5087–5092.
[13] J.J. Łucejko, F. Modugno, E. Ribechini, D. Tamburini, M.P. Colombini, Appl. Spectrosc. Rev. 50 (2015) 584–625.
[14] S. Krauss, W. Wagermaier, J.A. Estevez, J.D. Currey, P. Fratzl, J. Struct. Biol. 175 (2011) 457–464.
[15] A.A. Poundarik, A. Boskey, C. Gundberg, D. Vashishth, Sci. Rep. 8 (2018) 1191.
[16] C.d.C.A. Lopes, P.H.J.O. Limirio, V.R. Novais, P. Dechichi, Appl. Spectrosc. Rev. 53 (2018) 747–769.
[17] C.J. Kennedy, W.A. Revie, L. Troalen, M. Wade, T.J. Wess, Polym. Degrad. Stab. 98 (2013) 894–898.
[18] C.A.C. Crusciol, D.P. de Arruda, A.M. Fernandes, J.A. Antonangelo, L.R.F. Alleoni, C.A.C.d. Nascimento, O.B. Rossato, J.M. McCray, Sci. Rep. 8 (2018) 393.
[19] P. Milczarek, M. Zielinski, M.L. Garcia, Colloid Polym. Sci. 270 (1992) 1106–1115.
[20] R.L. McMullen, J. Jachowicz, J. Cosmet. Sci. (1998) 223–244.
[21] B.J. Teerink, Hair of West-European Mammals: Atlas and Identification Key, first ed., Cambridge Univ. Pr, Cambridge, 1991.
[22] S. Senthilkumar, R. Gnanadevi, T.A. Kannan, C.S. Arunaman, G. Ramesh, J. Entomol. Zool. Stud. 6 (5) (2018) 1925–1929.
[23] MicrolabNW Photomicrograph Gallery, Photographic gallery of hair, http://www.microlabgallery.com/hair.aspx, last access: 2019-12-29.
[24] B.C. Smith, Infrared Spectral Interpretation: a Systematic Approach, CRC Press, Boca Raton, 1999.
[25] Y. Kajiura, S. Watanabe, T. Itou, K. Nakamura, A. Iida, K. Inoue, N. Yagi, Y. Shinohara, Y. Amemiya, J. Struct. Biol. 155 (2006) 438–444.
[26] B. Hammouda, J. Appl. Crystallogr. 43 (2010) 716–719.
[27] K.R. Smith, D.M. Thiboutot, J. Lipid. Res. 49 (2008) 271–281.
[28] M. Ottaviani, E. Camera, M. Picardo, Mediat. Inflamm. 2010 (2010) 858176.
[29] R.L. McMullen, G. Zhang, T. Gillece, J. Cosmet. Sci. 66 (2015) 379–409.
[30] M. Machado, J. Hadgraft, M.E. Lane, Int. J. Cosmet. Sci. 32 (2010) 397–409.
[31] P. Pienpinijtham, C. Thammacharoen, S. Naranitad, S. Ekgasit, Spectrochim. Acta A Mol. Biomol. Spectrosc. 197 (2018) 230–236.
[32] E.O. Espinoza, B.W. Baker, T.D. Moores, D. Voin, Endang. Species Res. 9 (2010) 239–246.
[33] A.R.M. Müllner, R. Pahl, D. Brandhuber, H. Peterlik, Molecules 25 (2020) 2143.
[34] J. Tintner, F. Reiter, E. Smidt, B. Hinterstoisser, Cellul. Chem. Technol. 52 (1–2) (2018) 105–111.
[35] R.A. Blanquette, Deterioration in historic and archaeological woods from terrestrial sites, in: R.J. Köstler, Köstler Victoria R., A.E. Charola, F.E. Nieto-Fernandez (Eds.), Art, biology, and conservation: Biodeterioration of works of art; [the papers in this volume were presented at the "Art, Biology, and Conservation 2002 meeting" held at the Metropolitan Museum of Art, June 13 - 15, 2002], New York NY, Metropolitan Museum of Art, 2003, pp. 328–347.
[36] D. Istrate, C. Popescu, M.E. Rafik, M. Möller, Polym. Degrad. Stab. 98 (2013) 542–549.
[37] R. Vargiolu, C. Pailler-Mattei, M. Coudert, Y. Lintz, H. Zahouani, J. Archaeol. Sci. 40 (2013) 3686–3692.
[38] N. Kissi, K. Curran, C. Vlachou-Mogire, T. Fearn, L. McCullough, Herit. Sci. 5 (2017) 20.
[39] M. Călin, D. Constantinescu-Aruxandei, E. Alexandrescu, I. Răut, M.B. Doni, M.-L. Arsene, F. Oancea, L. Jecu, V. Lazăr, Electron. J. Biotechnol. 28 (2017) 101–112.
[40] G.A. Goodfriend, Nature 357 (1992) 399–401.